# A FULLY COUPLED GEOCHEMICAL MODEL WITH A PORE SCALE LATTICE BOLTZMANN SIMULATOR - PRINCIPLES AND FIRST RESULTS

Aksel Hiorth[1,2], Espen Jettestuen[1], Lawrence M. Cathles [3],
Reidar I. Korsnes [2], Merete V. Madland[2]
[1]IRIS – Petroleum, P. O. Box 8046, N-4068 Norway
[2]Department of petroleum, University of Stavanger, 4036 Stavanger
[3] Department of Earth and Atmospheric Sciences
Cornell University, Ithaca, New York 14853, Cornell University,

*This paper was prepared for presentation at the International Symposium of the Society of Core Analysts held in Halifax, Nova Scotia, Canada, 4-7 October, 2010*

## ABSTRACT

A fully coupled reactive transport model at pore-scale has been developed using the lattice Boltzmann algorithm and a geochemical model describing the chemical interactions at the pore wall. The purpose of this development is to shed more light on the effect of aqueous chemistry on the chemical and physiochemical properties of the pore space. Rate dependent mineral dissolution and precipitation, and induced changes in surface potential and charge due to the injected water have been studied. The model is compared with experiments, and it reproduces the experimental trends quite successfully.

## INTRODUCTION

Low salinity water flooding [1-4], spontaneous imbibition of seawater into mixed wet chalk [5-8], water weakening of chalk in the presence of magnesium rich brines [9], clearly demonstrate the effect of chemistry on the flow of oil and water in porous media. Chemical reactions in the water phase and at the pore wall can induce mineral precipitation, dissolution, changes in surface charge and potential. Some of the mentioned chemical or physiochemical changes of the pore surface may be relevant for understanding the mechanism behind wettability change or the water weakening effect. In order to fully understand the mechanism, systematic experiments and modelling at the pore scale must be performed.

The purpose of this paper is to present a geochemical model that has been coupled with a lattice Boltzmann (LB) simulator for fluid transport at the pore scale. Any number of chemical components (basis species) in the water phase can be specified (limited only by the computational time). For each of the components in the water phase a mineral or gas buffer can be specified. At the fluid mineral interface (pore wall) rate equations for dissolution and precipitation are used. In this paper we focus on the carbonate chemistry as the data are available to us.

Recently pore scale models have been developed using finite volume methods [10], and LB methods [11] in order to study $CO_2$ storage. The integrated LB model with geochemistry used in this paper has been developed at IRIS. The code can be run in 2D and 3D, however in this paper we only use the 2D option. The geochemical database has been adopted from EqAlt [8, 12], the geochemical model is comparable with PHREEQC [13] when it comes to the number of basis species and minerals present. Contrary to PHREEQC, our model can be used for high pressures and temperatures [14].

## LATTICE BOLTZMANN ALGORITHM FOR ADVECTION DIFFUSION AND FLUID FLOW

The physical system can be divided into three computational domains: 1) bulk fluid, 2) solid, and 3) walls, the boundary between fluid and solid nodes. The walls are where the interaction between the diffusion-advection solver and the geochemical solver takes place. This is done through a boundary condition that we will discuss later. The fluid flow and diffusion are simulated with the lattice Boltzmann method[15, 16]. This method has its basis in the microscopic behaviour of gases (and liquids), and the macroscopic dynamics are derived through an up scaling of this behaviour. The basic equation is the Boltzmann equation:

$$\frac{\partial f}{\partial t}(\vec{x},\vec{v},t)+\vec{v}\cdot\nabla f(\vec{x},\vec{v},t)=Q, \qquad (1)$$

where $f(\vec{x},\vec{v},t)$ is the probability density for finding a particle with velocity, $\vec{v}$, at the spatial coordinate, $\vec{x}$, at time, $t$. The left hand side of the equation can be regarded as a simple streaming of the probability density, which represents the free movement of particles. The right hand side of the equation represents the collision/interaction between particles and is usually referred to as the "collision operator".

One numerical scheme for solving this equation is the lattice Boltzmann method, which evolved from the lattice gas automata. The basic philosophy is to partition space into one of the standard lattice types (in this work we use the 2DQ9 lattice), and then choose a discrete set of velocities which follow the lattice directions. The collision operator is approximated by using the BGK operator [17] and the low Mach number limit of the equilibrium velocity distribution is used.

The numerical scheme is a discretization of the Boltzmann equation with the BGK approximation for the collision operator, $Q=-1/\tau(f-f^{eq})$,

$$f_i(\vec{x}+\vec{e}_i,t+1)-f_i(\vec{x},t)=-\frac{1}{\tau}(f_i(\vec{x},t)-f_i^{eq}), \qquad (2)$$

where the index, $i$, indicates the velocity basis, $\vec{e}_i$ is the lattice basis for the $i$'th direction, $f_i$ is the discretized version of the velocity distribution, and $f_i^{eq}$ is the equilibrium distribution and is evaluated from the macroscopic variables. The up scaling consists of identifying the macroscopic quantities for the density and velocity. The density at a given position $\vec{x}$ is simply the sum of $f_i$ for all velocity directions $i$. The

velocity is defined in a similar manner, where the $f_i$'s are multiplied with their corresponding velocity vector, $\vec{c}_i$:

$$m(\vec{x},t)=\sum_i f_i \qquad \text{and} \qquad m\vec{v}(\vec{x},t)=\sum_i f_i\vec{c}_i \tag{3}$$

The equilibrium distribution is derived from the Maxwell-Boltzmann velocity distribution in the low Mach number limit. The form of this expression is:

$$f_i^{eq}=\omega_i m\left(1+3\frac{\vec{c}_i\cdot\vec{u}}{c^2}+\frac{9}{2}\frac{(\vec{c}_i\cdot\vec{u})^2}{c^4}-\frac{3}{2}\frac{\vec{u}^2}{c^2}\right), \tag{4}$$

where $c$ is the "lattice sound speed".

The up scaling of the LB equation is formally derived through a multi-scale expansion, where the small parameter is identified as the Knudsen number. Assuming that the $f_i$'s only respects the first identity given in equation ( 3 ) and that the velocity in the equilibrium distribution ( $f^{eq}$ ) is given extrinsically, then equation ( 2 ) reproduces the advection diffusion equation:

$$\frac{\partial m}{\partial t}+\nabla\cdot(\vec{u}m)=D\nabla^2 m \quad \text{where } D=\frac{1}{3}(\tau-\frac{1}{2}), \tag{5}$$

Requiring that $f_i$ respects both relations in equation ( 3 ), the asymptotic of the LB equation is the incompressible Navier-Stokes equation:

$$\frac{\partial\vec{u}}{\partial t}+(\vec{u}\cdot\nabla)\vec{u}=-\frac{1}{\rho}\nabla p+\nu\nabla^2\vec{u}, \tag{6}$$

where $\rho$ is the now constant fluid density, $p$ is the pressure and $\nu=1/3(\tau-1/2)$ is the kinematic viscosity.

The boundary condition for the aqueous phase is set to no slip. This is enforced by a bounce back boundary condition, that is, the velocity distribution at the boundary is reversed.

## AQUEOUS AND SURFACE CHEMISTRY

The fluid part of the LB simulations defines the advective velocity field given by pressure differences in the porous rock. The velocity field is then used by the advection diffusion solver to predict the evolution of the concentrations of aqueous chemical species. The reactions take place at the boundary (wall) nodes where a varying number of minerals are present and surface sites for adsorption.

The mathematics of the geochemical computation is simplified by the introduction of basis species and secondary species (or complexes) [18]. Once the concentration of the basis species and dissociation constants (log Ks) are known the secondary species (complexes) can be calculated. In our implementation [12] we determine the dissolution and dissociation constants from the HKF equation of state [19-21] using thermodynamic data in the SUPCRT database [14]. For a recent review of the HKF equation of state, see

[22]. The concentration of other complexes can be calculated from the following disassociation reactions:

$$\begin{aligned} CO_3^{2-} &\rightleftharpoons HCO_3^- - H^+, \\ H_2CO_3 &\rightleftharpoons HCO_3^- + H^+, \\ CaSO_4^0 &\rightleftharpoons Ca^{2+} + SO_4^{2-}, \\ MgSO_4^0 &\rightleftharpoons Mg^{2+} + SO_4^{2-}, \\ >CO_3Mg^+ &\rightleftharpoons >CO_3^- + Mg^{2+}. \\ &\vdots \end{aligned} \qquad (7)$$

Note that the disassociation reactions above are a subset of the reactions considered in the geochemical model. If all the activities of the basis species on the right hand side are known, the concentration of the secondary species on the left hand side can be calculated. > indicates that the basis species are a surface species, i.e. located at the calcite mineral surface. The concentrations of the complexes can be determined by using the law of mass action, e.g. consider the second last equilibrium in equation ( 7 ):

$$a_{MgSO_4} = \frac{a_{Mg}\, a_{SO_4}}{K_{MgSO_4^0}}. \qquad (8)$$

The activities are related to the concentrations in the following way:

$$a_i = m_i \gamma_i, \quad \log_{10}\gamma_i = \frac{Z_i^2 A(T)\sqrt{I_0}}{1 + a_o B(T)\sqrt{I_0}}, \text{ and } I_o = \frac{1}{2}\sum_i Z_i^2 m_i. \qquad (9)$$

$m_i$ is the concentration of ion $i$, $\gamma_i$ is the corresponding activity coefficient, and A and B are functions that depend on the temperature [21]. $Z_i$ is the valence of the i'th species and $I_o$ is the ionic strength.

Calculation of the concentration of the surface complexes, e.g. the last equilibrium in equation ( 7 ), is a bit more involved as it is dependent on the surface charge and potential. For the calcite surface, surface charge is simply the sum of all the charged surface complexes [8, 23]:

$$\sigma = \frac{F}{S}\left(m_{>CaOH_2^+} - m_{>CaCO_3^-} - m_{>CaSO_4^-} - m_{>CO_3^-} + m_{>CO_3Mg^+}\right), \qquad (10)$$

where σ is the surface charge, F is Faradays constant, and S is the specific surface area ($m^2$/l). The surface potential is related to the surface charge by the Grahame equation [24]:

$$\sigma^2 = 2\varepsilon\varepsilon_0 k_B T\left(\sum_i m_i \exp\{-Z_i F\psi/(RT)\} - m_i\right), \qquad (11)$$

$\varepsilon_0$ is the dielectric constant of vacuum and ε is the dielectric constant of water, $k_B$ is the Boltzmann's constant, and R is the ideal gas constant. Once the surface charge is known, the concentration of the surface complexes can be calculated:

$$a_{>CO_3Mg} = \frac{a_{Mg} e^{-2F\psi/RT}\, a_{>CO_3}}{K_{>CO_3Mg}}. \qquad (12)$$

The physical meaning of the >CO3Mg+ complex is that it gives the total amount of adsorbed magnesium at the calcite surface. In the simulations, we make the following assumptions 1) No rate effects are involved in formation of the secondary complexes, e.g. equation ( 7 ) 2) The activity of H+ is determined by charge balance:

$$\sum_i Z_i m_i = 0 , \qquad (13)$$

and 3) The activity of $H_2O$ is equal to one. Assumption 1-2 has the direct consequence that the secondary species and the $H^+$ concentration does not need to be visible for the fluid part of the LB code. Only the total concentration of the basis species needs to be transported inside the pore space. In addition to the equations above, minerals can dissolve or precipitate.

## BOUNDARY CONDITIONS

The total concentrations of the basis species are known inside the pore space. The chemical reactions are limited to the pore boundaries, thus the chemical solver is only called at each boundary node. The only input needed for the chemical solver is the total concentrations of the basis species and the type and amount of minerals present at the pore wall. In this work we use a simple linear kinetic rate equation for mineral dissolution or precipitation:

$$\frac{dm_i^{Tot}}{dt} = k\left(m_i^{Tot,eq} - m_i^{Tot}\right). \qquad (14)$$

where $m_i^{Tot}$ is the total concentration of the i'th basis species, and $m_i^{Tot,eq}$ is the total equilibrium concentration of that species. $k$ is a rate constant that has to be determined from experiments. $m_i^{Tot,eq}$ is calculated by the chemical solver.

The algorithm is best illustrated with an example; a 0.219M $MgCl_2$ solution is injected into a chalk core (high concentration of calcite). In the simulations we assume that only calcite is present initially, at each boundary node the total concentration of $Ca^{2+}$, $Mg^{2+}$, $HCO_3^-$, and $Cl^-$ is known. The chemical solver is called; first it calculates the equilibrium concentration with only calcite present as the mineral phase, then it checks if some minerals are supersaturated. In this case magnesite is supersaturated, and thus it is expected to be formed. Then a second calculation is performed with magnesite present, $m_i^{Tot,eq}$ is calculated and the total concentration of the basis species are updated according to equation ( 14 ). One may argue that it is unlikely that all the concentrations at one boundary node should be updated at the same rate. This is true, but inside a porous media one of the reactions, e.g. calcite dissolution could be the rate limiting reaction and then one would expect the other reactions to proceed at a rate controlled by e.g. calcite dissolution, as indicated by equation ( 14 ).

## LB IMPLEMENTATION OF THE BOUNDARY CONDITION

The implementation of the boundary conditions follows the structure of [25]. The continuum linear kinetics boundary condition is given by:

$$D\vec{n}\cdot\nabla m + k\cdot\left(m - m^{eq}\right) = 0\,, \tag{15}$$

where $\vec{n}$ is the surface normal, $D$ is the constant of diffusion, $k$ is the rate and $m^{eq}$ is the equilibrium of the given species at the wall. The representation of this boundary condition in the LB frame work is:

$$\vec{c}_i\cdot\nabla f_i^{eq} = -\frac{C_2 c^2}{D}\left(f_i - f_i^{eq}\right)\,, \tag{16}$$

where $C_2$ is a constant depending on the lattice structure. Using that the fluid velocity at the boundary is zero in equation ( 4 ) we get that $f_i^{eq} = \omega_i m$, and this leads to the boundary condition

$$f_{-i} = (\chi - 1)f_i + (2 - \chi)\omega_i m^{eq} \tag{17}$$

where '$-i$' represent the reversed direction of $i$ and $\chi = 2\cdot\left(1 + k/C_2 c\right)^{-1}$. $m^{eq}$ is given by the chemical solver described above and is based on the rock surface minerals and the aqueous species concentrations at the surface.

## TEST OF THE CHEMICAL SOLVER

The chemical solver can be checked by comparing with PHREEQC [13]. As there is no pressure dependent database in PHREEQC we compare our chemical solver with PHREEQC at 50°C and 1 atm. The simulation example is simply a beaker with the initial solution given to the left in Table 1, dolomite and calcite is then added to the beaker and the solution equilibrate with the minerals present. The system is closed to the atmosphere (i.e. no equilibrium with CO2(g)). The other columns in Table 1 list the final equilibrium concentrations. We clearly see some spread in the calculated concentrations, which is mainly due to the different databases for the disassociation and dissolution logK values. Our calculation (the column to the right) lies somewhere in between the PHREEQC values. In Table 2 some of the major complexes are listed for the same calculation.

**Table 1:** Comparison of the chemical solver with PHREEQC, the concentrations are in M(mol/l). Initial phases are dolomite and calcite, five different databases has been run in PHREEQC. PHREEQC input file can be downloaded from http://www.ux.uis.no/~ah/comparison.phrq.

| Solution Species | Initial Solution | PHREEQC (llnl) | PHREEQC (minteq) | PHREEQC (phreeqc) | PHREEQC (pitzer) | PHREEQC (wateq4f) | LB Solver |
|---|---|---|---|---|---|---|---|
| $Ca^{2+}$ | 1.00E-08 | 2.10E-01 | 1.26E-01 | 1.53E-01 | 1.63E-01 | 1.53E-01 | 2.09E-01 |
| $Mg^{2+}$ | 2.19E-01 | 8.98E-03 | 9.35E-02 | 6.62E-02 | 5.61E-02 | 6.62E-02 | 1.02E-02 |
| $HCO_3^-$ | 1.00E-08 | 1.92E-05 | 5.09E-05 | 5.10E-05 | 3.13E-05 | 4.99E-05 | 3.14E-05 |
| $Cl^-$ | 4.38E-01 | 4.38E-01 | 4.38E-01 | 4.38E-01 | 4.38E-01 | 4.38E-01 | 4.38E-01 |
| pH | - | 8.12 | 7.79 | 7.74 | 7.82 | 7.74 | 7.83 |

**Table 2:** Some of the major complexes in the calculation.

| Solution complex | PHREEQC (llnl) | PHREEQC (minteq) | PHREEQC (phreeqc) | PHREEQC (pitzer) | PHREEQC (wateq4f) | LB Solver |
|---|---|---|---|---|---|---|
| $CaCl^+$ | 4.70E-03 | - | - | - | - | 4.52E-03 |
| $MgCl^+$ | 8.41E-04 | - | - | - | - | 8.51E-04 |
| $CaCl_2^0$ | 8.12E-04 | - | - | - | - | 6.17E-04 |
| $CaOH^+$ | 1.31E-06 | 5.29E-06 | 4.41E-07 | - | 4.38E-07 | 1.04E-05 |
| $CaHCO_3^+$ | 4.43E-06 | 1.54E-05 | 1.40E-05 | - | 1.27E-05 | 8.54E-06 |
| $OH^-$ | 1.03E-05 | 5.74E-06 | 4.75E-06 | 1.78E-07 | 3.83E-06 | 7.82E-06 |

## COMPARISON WITH EXPERIMENTS

The experimental data, which we will simulate, are those published in [9], where Liege chalk outcrop cores were flooded at 1PV/day with 0.219M $MgCl_2$ brine at 130°C, and with distilled water (DW) initially present in the cores. The effluent was analyzed during the experiment. When setting up the simulation, we need to specify the geometry. Inside a single pore, the concentration of the chemical species is uniform. This can be seen by calculating the Péclet number for the pore, which is defined as the ratio between the rate of advection to the rate of diffusion:

$$Pe = \frac{L\,u}{D} = \frac{1\mu m \cdot 0.81\,\mu m/s}{7000\mu m^2/s} = 3\cdot 10^{-5}. \qquad (18)$$

L is the characteristic length scale (in this case set equal to the pore size). u is the Darcy flow velocity, 1 pore volume/day or u = 7cm/day = 0.81 μm/s. D is the diffusion constant, and since the experiments were performed at 130°C we set $D=7\cdot 10^{-9}$ $m^2/s$. $Pe << 1$ indicates that diffusion will smear out all concentration gradients inside a pore. Based on this observation, we argue that the detailed pore structure is of minor importance, and a bundle of (2D) tubes model would be a good representation of the core. We will discuss the limitation of this assumption at the end. When setting up the simulation, the only constraint is thus that the Péclet number is the same in the simulations as in the experiments. Using L=7cm (the core length), equation ( 18 ) gives a Péclet number of 8. In the LB simulations the Péclet number is:

$$Pe = \frac{N_x\,u_{LB}}{\frac{1}{3}\left(\tau - \frac{1}{2}\right)} = 6N_x u_{LB}, \qquad (19)$$

note that in the last equation we have used τ=1. In the simulations we use $N_x$=40 (and τ=1), thus $u_{LB} = 0.033$ in order to have a Péclet number of 8. The simulation time step can be related to physical time by the following considerations:

$$u_{LB}\frac{\delta_x}{\delta_t} = u \Rightarrow \delta_t = \frac{u_{LB}}{u}\delta_x = \frac{Pe}{6N_x u}\frac{L}{N_x} = \frac{Pe}{6N_x^2}\frac{L}{u} = \frac{8}{6\cdot 40^2}\frac{7\text{cm/day}}{7\text{cm}} = 1.2\,\text{min}. \qquad (20)$$

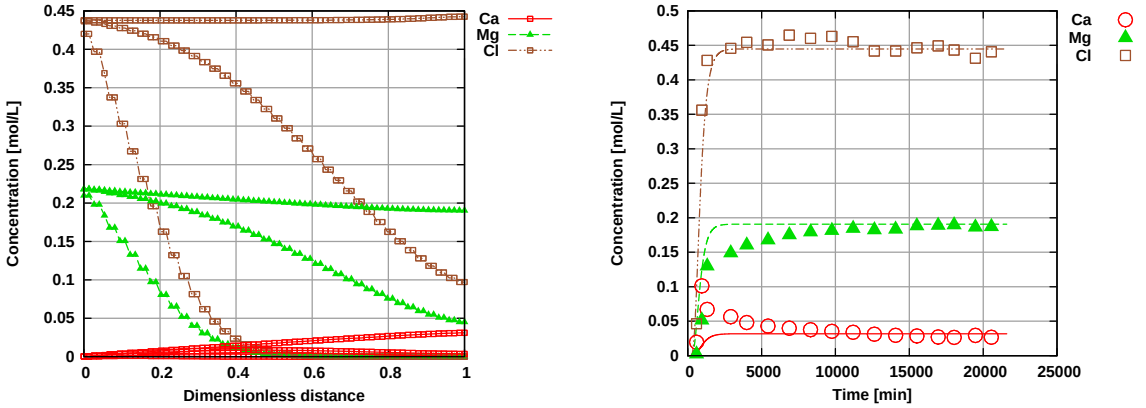


**Figure 1: (Left) Concentrations inside the tube (along the core), three different times 120 min, 480 min, and at long time (steady state), when 0.219M $MgCl_2$ is constantly injected at 1PV/day, DW is present initially. The concentrations are increasing along the core, as time increases. The chloride concentration is constant at steady state, as expected. The magnesium and calcium concentrations are decreasing and increasing respectively along the tube. (Right) Comparison between simulated (lines) and experimental (points) measured effluent concentrations.**

In Figure 1 the result of the simulation is shown, the only parameter that has been adjusted is the rate constant ($k=2.8\cdot10^{-3}$ /min). The match with the experimental data is striking, only one parameter has been adjusted (the rate constant). However, during the first period in the experiment there is an increase in the calcium production and a corresponding loss in magnesium. This is not captured by the model; calcium concentration reaches a level of 0.1M, and then it goes down to a steady state value of 0.03M. By multiplying the concentration profile with the flow rate, and integrating from 800 min to 13000 min, we can estimate the difference between the model and experimental data to be 0.0040 mol. Thus there is 0.0040 mol $Ca^{2+}$ that can not be accounted for by the model. Could this be due to adsorption/desorption? If we assume that there are 2 adsorption sites/$nm^2$ [8], surface area for chalk of $2m^2/g$, and a mass of the core to be 100g [9], we can estimate the number of adsorption sites to 0.00066 mol. Even if all the sites were occupied with calcium and then replaced by magnesium it is not enough to explain the extra calcium production. At least two other mechanism could account for the extra calcite production 1) Some fast dissolving calcite could be present in the core (e.g. smaller crystals with high surface area), this hypothesis can be used when modelling quartz/feldspar rock[26] 2) When magnesite precipitates it inhibits the calcite dissolution. Thus the dissolution is fast initially and slows down when magnesite precipitates. The first possibility can be investigated if we simply assume that 4% of the core consists of calcite that will dissolve faster, the result is shown in Figure 2. The peak is reproduced, but not the transient phase.

Magnesium is known to inhibit the dissolution rate of calcite at the pH range 8-9 [27]. The effect of magnesium can be included in the model by allowing the rate constant to be dependent on the magnesite concentration at the surface:

$$k \to k_1 \left( \frac{1 + k_2 \, c_{\text{magnesite}}}{1 + k_3 \, c_{\text{magnesite}}} \right), \qquad (21)$$

where $c_{magnesite}$ is the concentration of magnesite at the rock surface. Adjusting the parameters, we find the result shown in **Figure 3**. The transient behaviour is now captured much better by the model.

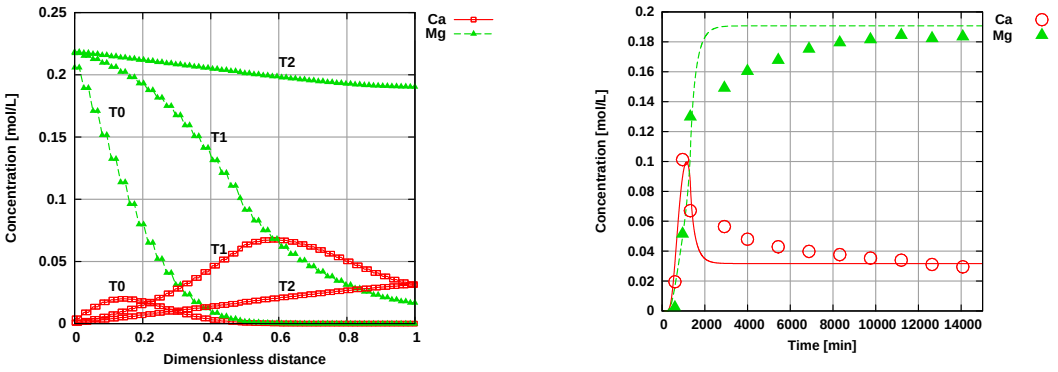


**Figure 2: (Left) Concentrations inside the tube (along the core) at three different times $T_0$=120 min, $T_1$=480 min, and at steady state ($T_2$), when 0.219M $MgCl_2$ is constantly injected at 1PV/day, DW is present initially. There is a wave of calcium transported along the core, the long time steady state concentration is lower than during the transient period. (Right) Comparison between simulated (lines) and experimental (points) measured effluent.**

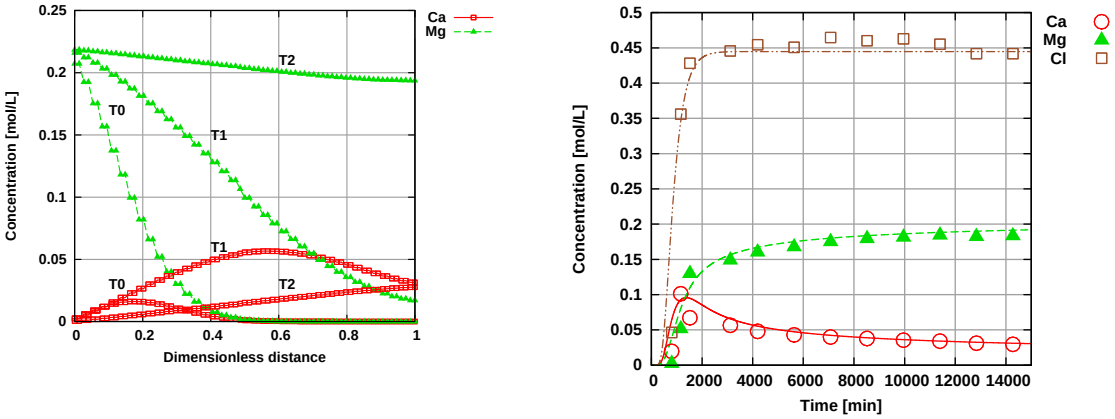


**Figure 3: (Left) Concentrations inside the tube (along the core) at three different times $T_0$=120 min, $T_1$=480 min, and at steady state ($T_2$) , when 0.219M $MgCl_2$ is constantly injected at 1PV/day, DW is present initially. There is a wave of calcium transported along the core, the long time steady state concentration is lower than during the transient period. Comparison between simulated (lines) and experimental (points) measured effluent for the case of magnesium inhibition of calcite dissolution. The parameters are k1=0.25/min, k2=0.05 l/mol, k3=15 l/mol.**

## SURFACE CHARGE AND POTENTIAL

The LB code has an option where it is possible to add surface species, in this paper we keep the number of calcium and carbonate surface sites constant, and equal to 2

sites/(nm)$^2$. They are not changed even if a new mineral precipitates. In Figure 4 the surface potential and charge is shown. As the magnesium front moves into the core, magnesium is adsorbed and the surface charge increases. The surface potential is inversely proportional to the ionic strength and that explains why it is higher initially (only distilled water is present initially). To the right in Figure 4 we see the adsorbed calcium and magnesium concentrations (note that the scale is mmol/L). The adsorbed magnesium concentration follows closely the surface charge as expected.

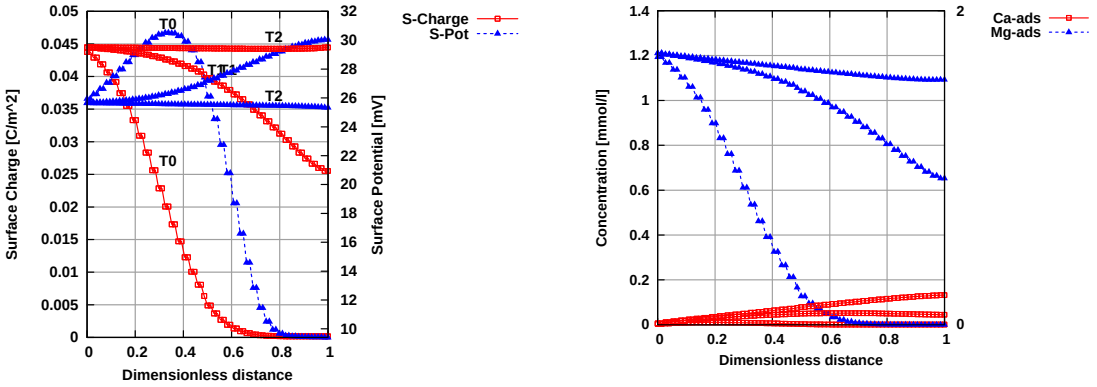


**Figure 4: (Left) Surface potential and surface charge inside the tube (along the core) at three different times when 0.219M $MgCl_2$ is constantly injected at 1PV/day, DW is present initially. (Right) The corresponding adsorption of magnesium and calcium inside the core as a function of time. The lines correspond to different times $T_0$=120 min, $T_1$=480 min, and at steady state ($T_2$). Note that this is the case with no fast dissolving calcite or inhibition of calcite dissolution due to magnesite.**

## CONCLUSION

A LB model integrated with a geochemical model has been presented, the chemical model has been compared with PHREEQC [13]. We have demonstrated that the LB model can be compared with experimental data [9], hypothesis can be tested, such as the presence of fast dissolving calcite and inhibition of calcite dissolution by precipitation of magnesite. The model reproduces the effluent curves observed in the experiment, and it gives additional information such as the surface charge and potential. The full potential of the model has not been explored in this paper. In particular no physical interpretation is found for the parameters in equation ( 21 ). Using a pore geometry with correct surface to volume ratio, and allow for the possibility of newly precipitated minerals to cover old ones might be a way of justifying equation ( 21 ). In the LB model it is easy to change the surface characteristics, such as the wetting state of the surface based on the calculated changes in the chemical or physiochemical parameters. By including a second non miscible phase, makes it possible to use this model to investigate suggested mechanisms for wettability change [7, 8].

## ACKNOWLEDGEMENTS

The authors acknowledge BP Norge and the Valhall co-venturers, including Hess Norge AS, A/S Norske Shell, and Total E&P Norge AS, ConocoPhillips and the Ekofisk co-venturers, including TOTAL, ENI, StatoilHydro and Petoro for financial support.

## REFERENCES

1. G.Tang and N.R. Morrow, *Oil Recovery by Waterflooding and Imbibition - Invading Cation Valency and Salinity.* SCA, 1999. **9911**.
2. Jerauld, G.R., et al., *Modeling low-salinity waterflooding.* the 2006 SPE Annual Technical Conf. & Exhib., San Antonio, Texas, U.S.A, 24-27 Sept., 2006. **SPE102239**.
3. Lager, L., et al., *Low salinity oil recovery - an experimental investigation.* SCA2006, 2006. **36**.
4. Yildiz, H.O. and N.R. Morrow, *Effect of brine composition on recovery of Moutray crude oil by waterflooding.* J. Pet. Sci. Eng., 1996. **14**: p. 159-168.
5. Zhang, P.M. and T. Austad, *Wettability and oil recovery from carbonates: Effects of temperature and potential determining ions.* Colloids and Surfaces a-Physicochemical and Engineering Aspects, 2006. **279**(1-3): p. 179-187.
6. Zhang, P.M., M.T. Tweheyo, and T. Austad, *Wettability alteration and improved oil recovery in chalk: The effect of calcium in the presence of sulfate.* Energy & Fuels, 2006. **20**(5): p. 2056-2062.
7. Evje, S. and A. Hiorth, *A Mathematical Model for Dynamic Wettability Alteration Controlled by Water-Rock Chemistry.* Networks and Heterogeneous Media, 2010. **5**(2): p. 217-256.
8. Hiorth, A., L.M. Cathles, and M.V. Madland, *The impact of pore water chemistry on carbonate surface charge and oil wettability.* Transport in Porous Media, 2010. **10.1007/s11242-010-9543-6**.
9. Madland, M.V., et al., *Rock Fluid Interactions in Chalk exposed to Injection of Seawater, MgCl2 and NaCl2 Brines with Equal Ionic Strength.* EAGE-2009, 2009. **A22**.
10. Flukiger, F. and D. Bernard, *A new numerical model for pore scale dissolution of calcite due to CO2 saturated water flow in 3D realistic geometry: Principles and first results.* Chemical Geology, 2009. **265**: p. 171-180.
11. Kang, Q., et al., *Pore Scale Modeling of Reactive Transport Involved in Geologic CO2 Sequestration.* Transport in Porous Media, 2009. **82**: p. 1573-1634.
12. Cathles, L.M. *EQAlt-Equilibrium Chemical Alteration*. in *Combined Physical and Chemical Geofluids Modeling*. 2006. University of Windsor, Windsor, Ontario.
13. Parkhurst, D.L. and C.A.J. Appelo, *User's guide to PHREEQC (version 2)-A computer program for speciation, batch-reaction, one-dimensional transport, and inverse geochemical calculations.* US Geol. Survey, Water-Resour. Inv. Rep., 1999. **99-4259**: p. (www.xs4all.nl/~appt).

14. Johnson, J.W., E.H. Oelkers, and H.C. Helgeson, *SUPCRT92: A software package for calculating the standard molal thermodynamic properties of minerals, gases, aqueous species, and reactions from 1 to 5000 bar and 0 to 1000 C.* Comp. and Geo. Sci., 1992. **18**(7): p. 899-947.
15. Succi, S., *The lattice Boltzmann equation, for fluid dynamics and beyond*. 2001: Oxford University Press.
16. Wolf-Gladrow, D.A., *Lattice-Gas Cellular Automata and Lattice Boltzmann models: an introduction*. 2000: Springer.
17. Chen, S. and G.D. Doolen, *Lattice Boltzmann method for fluid flows.* Annu. Rev. Fluid Mech., 1998. **30**: p. 329-364.
18. Bethke, C.M., *Geochemical Reaction Modeling*. 1966, New York: Oxford University Press.
19. Helgeson, H. and D. Kirkham, *Theoretical prediction of the thermodynamic behavior of aqueous electrolytes at high pressures and temperatures; II, Debye-Huckel parameters for activity coefficients and relative partial molal properties.* Am. J. Sci., 1974. **274**: p. 1089-1198.
20. Helgeson, H. and D. Kirkham, *Theoretical prediction of the thermodynamic behavior of aqueous electrolytes at high pressures and temperatures; I, Summary of the thermodynamic/electrostatic properties of the solvent.* Am. J. Sci., 1974. **274**: p. 1089-1198.
21. Helgeson, H., D. Kirkham, and G. Flowers, *Theoretical prediction of the thermodynamic behavior of aqueous electrolytes by high pressures and temperatures; IV, Calculation of activity coefficients, osmotic coefficients, and apparent molal and standard and relative partial molal properties to 600 degrees C and 5kb.* Am. J. Sci., 1981. **281**: p. 1249-1516.
22. Oelkers, E.H., P. Benezeth, and G.S. Pokrovski, *Thermodynamic Databases for Water-Rock Interaction.* Thermodynamics and Kinetics of Water-Rock Interaction, 2009. **70**: p. 1-46.
23. Van Cappelen, P., et al., *A surface complexation model of the carbonate mineral-aqueous solution interface.* Geochim. Cosmo. Acta, 1993. **57**: p. 3505-3518.
24. Israelachivili, J., *Intermolecular and Surface Forces*. 1985, New York City: Academic Press.
25. Hiorth, A., et al., *A lattice Boltzmann-BGK algorithm for a diffusion equation with Robin boundary condition-application to NMR relaxation.* International Journal for Numerical Methods in Fluids, 2009. **59**(4): p. 405-421.
26. Appelo, C.A.J., *PHREEQC-2 COURSE*. 2010.
27. Compton, R.G. and C.A. Brown, *The Inhibition of Calcite Dissolution/Precipitation: Mg2+ Cations.* Journal of Colloid and Interface Science, 1994. **165**(2): p. 445-449.